LIMNOLOGY and OCEANOGRAPHY

ASLO

Limnol. Oceanogr. 9999, 2024, 1–18

doi: 10.1002/lno.12493

Physiological and interspecific factors determine diel changes in phytoplankton bio-optical properties

Nicholas Baetge,[1,2*] **Kimberly H. Halsey**,[2] **Jason R. Graff**,[1] **Brian Ver Wey**,[1] **Toby K. Westberry**,[1] **Amanda E. Appel**,[2] **Guillaume Bourdin**,[3] **Charlotte Begouen Demeaux**,[3] **Emmanuel Boss**,[3] **Michael J. Behrenfeld**[1]

[1]Department of Botany and Plant Pathology, Oregon State University, Corvallis, Oregon, USA
[2]Department of Microbiology, Oregon State University, Corvallis, Oregon, USA
[3]School of Marine Sciences, University of Maine, Orono, Maine, USA

Abstract

Bio-optical properties of marine phytoplankton retrieved through satellite remote sensing are used to estimate ocean productivity and carbon cycling. Daily activity of phytoplankton is attuned to the predictable light fluctuations of the diel cycle. Field and laboratory studies have documented diel changes in phytoplankton growth, division, and respiration, carbon and pigment content, cell size, photosynthetic efficiency and rate, and DNA replication and transcription. Many of these physiological changes can alter cellular optical properties and contribute to diel variations in bulk absorption and scattering properties. Consequently, understanding phytoplankton contributions to diel optical cycles is essential for improving algorithms that convert remote sensing data to biological rates and stocks. Here, we describe time-resolved cellular, photophysiological, and bio-optical properties for three cultured phytoplankton ranging in cell size from ~ 1 to 6 μm: *Ostreococcus lucimarinus*, *Synechococcus* (WH8102), and *Thalassiosira pseudonana*, all of which can significantly contribute to phytoplankton abundance and/or biomass in the open and coastal ocean. This work is the first to characterize complete diel cycles in absorption and attenuation for *O. lucimarinus* and backscattering for all these species. Results show that the percent increase from the minimum to maximum values over the diel cycle ranged between ~ 24–121%, ~ 31–235%, and ~ 25–198% for particulate absorption, attenuation, and backscattering, respectively. Diel changes in bio-optical properties also differed in both timing and magnitude across phytoplankton species, demonstrating the importance of contextualizing remote sensing observations with phytoplankton community composition.

The submarine light environment is influenced by properties of resident phytoplankton populations, including cell concentration, size distribution, cell shapes, pigment composition, internal cellular structures, and cell refractive indices (Kirk 1975; Jerlov 1976). Attenuation, absorption, and scattering coefficients of phytoplankton are additive inherent optical properties (independent of the angular distribution and magnitude of the incident light field) needed in forward bio-optical models to interpret apparent optical properties (dependent on the angular distribution and magnitude of the light field) of seawater observed by satellite remote sensing (Morel and Prieur 1977; Bricaud et al. 1983). Knowing the contribution of phytoplankton absorption and scattering allows satellite measurements of water-leaving radiance to be used in inverse bio-optical models to monitor changes in phytoplankton biomass and production, which are critical for forecasting ocean food web and biogeochemical processes (Morel et al. 1991; Behrenfeld et al. 2005; Zaneveld et al. 2007).

The daily fluctuation of light in the surface ocean is an important environmental cue for phytoplankton. Many phytoplankton synchronize endogenous biological clocks with the daily light cycle to regulate and prevent induction of night-associated metabolic processes during ephemeral exposures to

*Correspondence: nicholasbaetge@gmail.com

Additional Supporting Information may be found in the online version of this article.

Author Contribution Statement: M.J.B., K.H.H., J.R.G., and E.B. conceived the study. N.B., M.J.B., K.H.H., J.R.G., T.W., E.B., G.B., and C.B. designed the experiments. N.B., K.H.H., J.R.G., B.V., A.E.A., and M.J.B. collected the samples. N.B. and B.V. processed the samples. NB analyzed the data and all authors assisted with data reduction and contributed to the revision and editing of the final manuscript.

darkness (e.g., cloud cover, storm-driven deep mixing) (Sournia 1975; Brand 1982). Existence of such endogenous clocks is demonstrated in laboratory phytoplankton cultures exhibiting periodicity in photosynthesis for > 70 h following transition from light to dark cycles to constant light (e.g., Brand 1982).

Field and laboratory studies document energy and carbon accumulation (e.g., carbohydrates and lipids) during the day in phytoplankton, with subsequent metabolism and respiration at night (Halsey and Jones 2015; Becker et al. 2018). Phytoplankton also exhibit diel changes in carbon content and volume (Olson et al. 1990; Stramski and Reynolds 1993; Durand and Olson 1996; DuRand et al. 2002), pigment content and composition (Yentsch and Ryther 1957; Owens et al. 1980), molecular composition (Cuhel et al. 1984; Becker et al. 2018), chloroplast shape and orientation (Herman and Sweeney 1975), photosynthetic efficiency and carbon fixation (Goldman et al. 1969; Harding et al. 1981), chlorophyll fluorescence (Brand 1982; Jacquet et al. 2001), and cell division (Armbrust et al. 1989; Jacquet et al. 2001).

Diel physiological cycles drive corresponding bio-optical cycles. For example, cell and/or carbon-specific attenuation coefficients are influenced more by changes in cellular refractive index than cell size for the diatom *Thalassiosira pseudonana* (Stramski and Reynolds 1993) and cyanobacterium *Synechococcus* (WH8103) (Stramski et al. 1995), while the opposite was observed for two small chlorophytes, *Nannochloris* and *Micromonas pusilla* (DuRand and Olson 1998; DuRand et al. 2002). Thus, understanding such species-specific dependences is essential for predicting bulk seawater optical properties from phytoplankton community composition (Ahn et al. 1992) and vice versa (Siegel et al. 1989; Stramska and Dickey 1992).

Diel cycles in bio-optical properties, namely absorption, attenuation, and scattering, have been observed for a range of cultured phytoplankton (Stramski and Reynolds 1993; Stramski et al. 1995; DuRand and Olson 1998; DuRand et al. 2002; Poulin et al. 2018). Building on this foundation, the current study reports complete diel cycles in backscattering coefficients alongside other cellular, physiological, and optical properties for *T. pseudonana*, *Synechococcus* (WH8102), and the chlorophyte *Ostreococcus lucimarinus*. These species were chosen to represent phytoplankton groups that are often numerically dominant in the ocean. Diatoms (e.g., *T. pseudonana*) often dominate nanophytoplankton (5–20 μm) biomass and abundance in upwelling and high latitude regions (Pierella Karlusich et al. 2020). *Synechococcus* and *Ostreococcus* often contribute significantly to picophytoplankton (≤ 2 μm) abundance and biomass in coastal and open ocean waters (Worden et al. 2004; Bolaños et al. 2020).

Cell- and carbon-specific changes in absorption, attenuation, and scattering have been observed to be related to changes in cellular refractive index and cell size (Stramski and Reynolds 1993; Stramski et al. 1995). Poulin et al. (2018) used *T. pseudonana* cultures to describe cell size- and abundance-dependent diurnal changes in backscattering. Here, we report the first complete diel cycles in bio-optical properties for *O. lucimarinus* and backscattering coefficients for *T. pseudonana* and *Synechococcus*. We show that (1) bio-optical properties co-vary with diel changes in cell physiology, (2) interspecific variability exceeds intraspecific variability in diel cycles of biomass-specific bio-optical properties, and (3) diel variations of biomass-specific beam attenuation and backscattering coefficients differ in amplitude and timing within and between species. These results are particularly relevant for understanding day–night differences in ocean optical properties observed with satellite lidar (e.g., Cloud-Aerosol Lidar with Orthogonal Polarization [CALIOP] sensor; Behrenfeld et al. 2019), but are also important for interpreting ocean color data from geostationary sensors and between polar-orbiting sensors with different equator crossing times.

Materials and methods

Culture growth conditions

F/2 + Si medium was used to grow *T. pseudonana* (Guillard and Ryther 1962), L1 medium to grow *Synechococcus* (Guillard and Hargraves 1993), and L1–Si medium to grow *O. lucimarinus*. All phytoplankton were maintained in semi-continuous growth by dilution every 1–2 d for at least 3 weeks to ensure cells were fully acclimated to their environment. During the weeks prior to the full suite of bio-optical sampling, cell concentrations were monitored once or twice daily at the same times of day and variable fluorescence was monitored to ensure consistent growth and physiology during diel sampling. Cultures were maintained in 1-liter polycarbonate bottles in a temperature-controlled room at 18°C under a 12 : 12-h light–dark sinusoidal light cycle. Light was provided using a custom light-emitting diode (LED) Phyto-panel (Photon Systems Instruments) composed of white and blue light LEDs. Irradiance ranged from total darkness to 390 μE m^{-2} s^{-1} and was measured with a 4π spherical quantum meter (Biospherical Instruments QSL-100) (Fig. 1a). All cultures were continuously bubbled with ambient air filtered through an activated charcoal hydrocarbon trap to keep cells in suspension and to prevent CO_2 limitation.

Diel experiments

Two independent experiments were conducted for each phytoplankton species within a week of each other and are summarized in Table 1. During each experiment, acclimated cultures were sampled every 2 h over the course of 24–28 h. While the total number of replicate cultures and sampled parameters varied between experiments, samples were always taken for flow cytometry and chlorophyll fluorescence to evaluate consistency between replicate cultures and experiments. In both *T. pseudonana* experiments, cultures were diluted to dawn cell concentrations at each measured time point after the onset of cell division 8 h after dawn to ensure sufficient

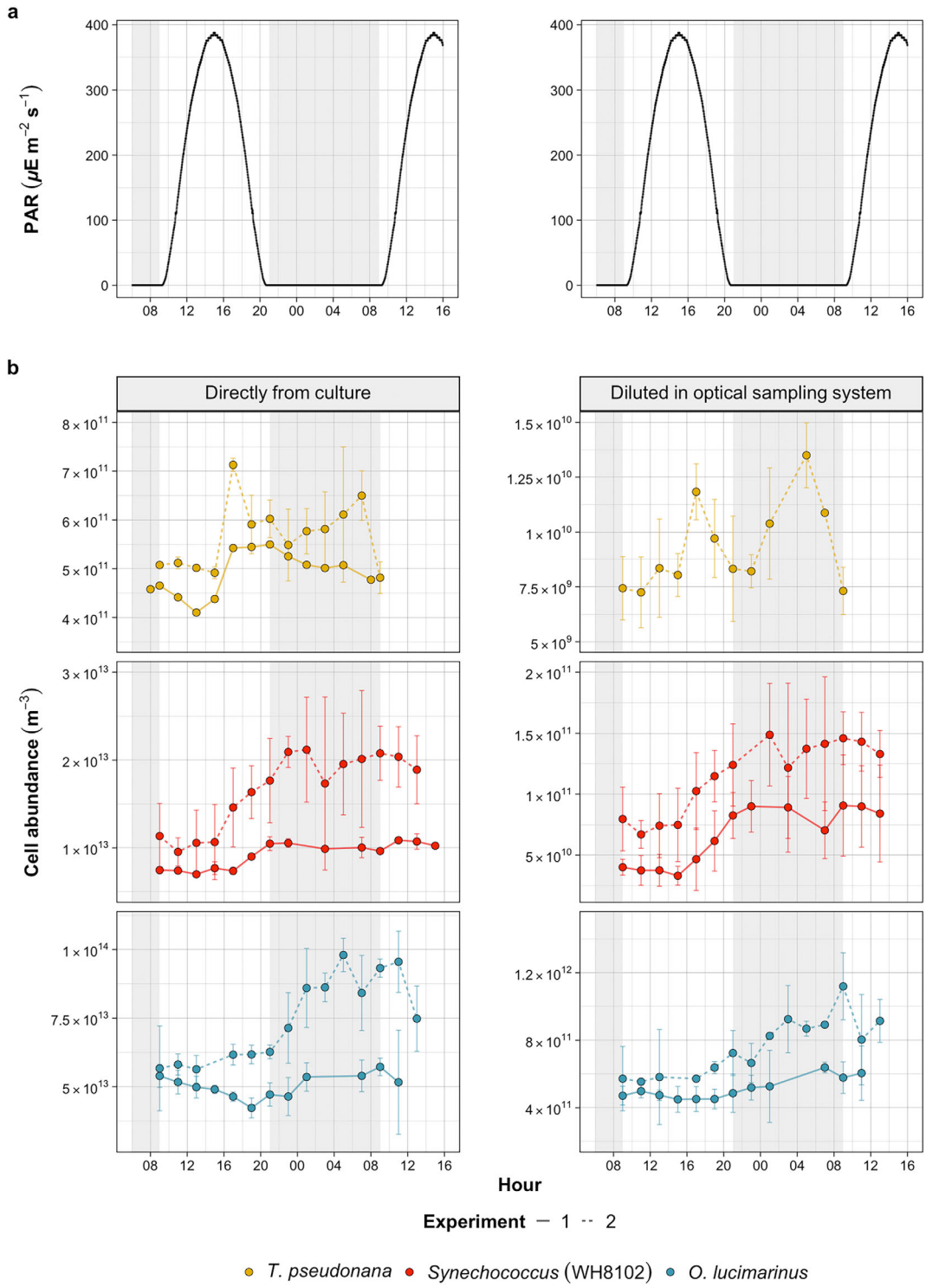

Fig. 1. Photosynthetically active radiation (PAR) over the 12 : 12-h light–dark sinusoidal light cycle for each phytoplankton culture (**a**). Mean cell abundances and their standard deviations for each diel experiment (**b**) measured directly from the cultures (left) and after dilution in the recirculating optical sampling system (right).

sampling volume for the duration of the experiments. *Synechococcus* and *O. lucimarinus* experiments were not diluted during the experiments as these species were maintained at cell densities 1–2 orders of magnitude higher than *T. pseudonana* and thus required less sample volume per sampling time point.

Table 1. Overview of cultures, replicates, and sampling scheme for each experiment. Mean growth rates (μ) and their standard deviations are reported for culture data following acclimation to growth conditions, including those taken for the diel experiments. Cell concentrations are reported for both the cultures and the recirculating sampling loop. At each sampling point of each experiment, volume from each culture replicate was diluted into the 3.8 liters residence volume of the recirculating sampling loop connecting the optical instruments.

							n culture replicates sampled for				Cell concentrations in	
Phytoplankton	μ (d^{-1})	Divisions (d^{-1})	Doubling time (d)	Experiment	Cultures (*n*)	*n* timepoints	Flow cytometry	Chlorophyll fluorescence	POC/PON	Optical properties	Cultures	Recirculating sampling loop
Thalassiosira pseudonana	0.95 ± 0.57 (median = 0.90, *n* = 50)	1.37	0.73	1	1	13	1	1	—	—	4.1×10^{11} to 5.5×10^{11}	—
				2	3	13	3	3	1 for 11 timepoints; 3 for 2 timepoints	3	4.8×10^{11} to 7.1×10^{11}	7.3×10^{10} to 1.4×10^{10}
Synechococcus (WH8102)	0.22 ± 0.66 (median = 0.38, *n* = 34)	0.31	3.2	1	2	16	2	2	—	2	7.0×10^{12} to 1.4×10^{13}	3.3×10^{9} to 9.1×10^{10}
				2	4	16	4	4	1 for 13 timepoints; 3 for 3 timepoints	3	9.5×10^{12} to $2.1 \times 10{-}^{13}$	6.7×10^{10} to 1.5×10^{11}
Ostreococcus lucimarinus	0.36 ± 0.67 (median = 0.18, *n* = 22)	0.52	1.9	1	3	12	3	3	—	3	4.2×10^{13} to 5.7×10^{13}	4.5×10^{11} to 6.4×10^{11}
				2	4	15	4	4	1 for 13 timepoints; 3 for 3 timepoints	3	5.6×10^{13} to 9.8×10^{13}	5.5×10^{11} to 1.1×10^{12}

Flow cytometry measurements

Samples of live phytoplankton cells were collected directly from cultures and from the recirculating optical sampling system following measurement of attenuation, absorption, and backscattering. These samples were immediately enumerated and analyzed using a Guava easyCyte 5HT flow cytometer (Millipore) with a 50-mW blue laser (488 nm), three bandpass filters (525 ± 30, 583 ± 26, and 695 ± 50 nm), and detectors for forward and side scattering (FSC and SSC, respectively). *T. pseudonana* and *O. lucimarinus* cell fluorescence was detected at 695 nm (chlorophyll fluorescence indicator), and *Synechococcus* fluorescence was detected at 583 nm (phycoerythrin fluorescence indicator).

Carbon and nitrogen

Particulate organic carbon (POC) and particulate organic nitrogen (PON) concentrations (mg C and N m^{-3}) were determined in triplicate from 5 to 6 mL culture volumes (5.4 ± 0.3 mL) filtered onto pre-combusted (450°C for 5 h) 25 mm Advantec GF75 filters (0.3 μm, nominal). Due to their small size, *Ostreococcus* were filtered through two stacked filters to increase filter cell retention. Filtrates were analyzed by flow cytometry to assess cell loss through filters. In filtrate samples where cells were detected ($n = 29$ of 191 samples), the total number of cells in the filtrate represented 1.1% ± 0.9% of the unfiltered cell count. Culture filtrates were also re-filtered onto GF75 filters to be analyzed for extracellular POC and PON background subtraction. Filters were immediately placed in storage at −20°C and subsequently dried at 60°C for 24 h, packed into tin capsules, and stored in a desiccator until analysis. Elemental composition was determined with an Exeter Analytical CE-440 Elemental Analyzer calibrated using acetanilide standards. Calculated POC and PON for each sample were normalized to the respective cell concentration (cells m^{-3}) and were also used to assess cellular carbon to nitrogen (C : N, mol : mol) and carbon to chlorophyll *a* (C : Chl *a*, weight : weight) ratios.

Chlorophyll fluorescence

Measurements of chlorophyll fluorescence yield when all functional PSII reaction centers are oxidized (F_o) and reduced (F_m) were made for each culture using a Soliense Light Induced Fluorescence Transient Fluorometer (LIFT-FRR) (Kolber et al. 1998). *Synechococcus* and *O. lucimarinus* samples were dark-acclimated for 5 min to relax non-photochemical quenching (NPQ) (Mackey et al. 2013; Halsey et al. 2014). *T. pseudonana* samples were low-light acclimated at 10–15 μEin m^{-2} s^{-1} prior to measurements because diatom NPQ does not fully relax in the dark (Milligan et al. 2012). For each sample, 200–300 μL of culture volume were diluted into 2 mL of 0.2-μm filtered artificial seawater and then measured in a glass cuvette within the LIFT-FRR. We followed the four-phase FRR excitation protocol described by Brown et al. (2019) and used data from the initial single-turnover phase to calculate the quantum efficiency of photochemistry (F_v/F_m) as (Maxwell and Johnson 2000):

$$\frac{F_v}{F_m} = \frac{(F_m - F_o)}{F_m} \quad (1)$$

Optical measurements

Hyperspectral absorption (*a*) and attenuation (*c*) of the cultures and 0.2-μm filtered culture water were measured at ~ 4 nm spectral resolution using an AC-S spectrophotometer (Sea-Bird Scientific [WET Labs, Inc.]; serial number 94). Simultaneous backscattering counts at three wavelengths (470, 532, and 660 nm) were measured using an ECO-BB3 sensor (Sea-Bird Scientific [WET Labs, Inc.]; serial number 349) set in a custom enclosure (Dall'Olmo et al. 2009). For each experiment, the AC-S and ECO-BB3 were connected by silicone tubing in a recirculating loop that was powered by a peristaltic pump (~ 60 mL min^{-1}), similar to Poulin et al. (2018). The total residence volume of the recirculating loop was 3.8 liters and was initially filled at the beginning of each experiment with 0.2-μm filtered artificial seawater. At each sampling point, volume from each culture replicate was added to the recirculating loop in series using a 60-mL syringe. The volume of culture added was previously determined such that it would provide a backscattering signal at least 20% higher than background. A 0.2-μm Polycap capsule filter (Whatman), flushed with 50 liters of nanopure water prior to first use, was used to remove cells between sampling points. Optical data for each sample were logged over 1 min using the open-source software, Inlinino (Haëntjens and Boss 2020), and median values were used in subsequent analyses.

Derivations from optical measurements

Particulate absorption (a_p) and attenuation (c_p) were estimated using a calibration-independent technique in which measurements of 0.2-μm filtered sample water were subtracted from unfiltered measurements (Slade et al. 2010). A semiempirical scattering correction was applied to particulate absorption and attenuation spectra following Röttgers et al. (2013), which was shown by Kostakis et al. (2021) to consistently perform well over a wide range of water types and with less error propagation relative to other correction methods. Particulate scattering (b_p) was estimated as the difference between attenuation and absorption. Temporal variability in a_p and c_p are presented for the wavelengths measured by the ECO-BB3 (470, 532, and 660 nm), which also correspond to previous reports (Stramski and Reynolds 1993; Stramski et al. 1995; Durand and Olson 1996; DuRand and Olson 1998; Claustre et al. 2002; DuRand et al. 2002; Poulin et al. 2018). However, hyperspectral a_p and c_p data are also presented in Supporting Information Fig. S1. Chl *a* concentrations (mg m^{-3}) were estimated from the particulate absorption line height at 676 nm ($Chl_{a(676)LH}$) following Roesler and Barnard (2013) using a chlorophyll-specific absorption value at 676 nm of 0.014 m^2 g Chl^{-1} (Boss et al. 2007):

$$\text{Baseline}(676) = \frac{a_p(676) - a_p(650)}{65} * 26 + a_p(650) \quad (2)$$

$$\text{Line height}(676) = a_p(676) - \text{baseline}(650) \quad (3)$$

$$\text{Chl}_{a(676)\text{LH}} = \frac{\text{line height}(676)}{0.014} \quad (4)$$

$\text{Chl}_{a(676)\text{LH}}$ was used to calculate C : Chl *a* ratios (weight : weight). Pigment analyses reported in the Supporting Information were conducted by unsmoothing and then decomposing particulate absorption spectra into component Gaussian functions following Chase et al. (2013).

Prior to each set of phytoplankton experiments, the ECO-BB3 was calibrated using the transmission-tube (c tube) of the AC-S and serial dilutions of 0.2- and 0.7-μm NIST-traceable polystyrene Nanosphere Size Standard beads (Thermo Scientific) in nanopure water. The volume scattering function (β) at 124° of the beads at different concentrations was measured and then theoretically modeled based on their particle size distribution and index of refraction using Mie theory (Sullivan et al. 2013). The calibration slope (m sr^{-1} $count^{-1}$) of the ECO-BB3 was computed as the ratio between the theoretical slope (sr^{-1}) and measured slope (counts m^{-1}) of β and *c*. The particulate portion of the volume scattering function (β_p, m^{-1} sr^{-1}) was calculated by subtracting the contribution from 0.2-μm filtered seawater (Slade et al. 2010). The particulate backscattering coefficient (b_{bp}) for each wavelength measured by the ECO-BB3 was computed using the conversion factor $\chi = 1.12$ derived from Sullivan and Twardowski (2009) as:

$$b_{bp} = 2\pi\chi\beta_p \quad (5)$$

Backscattering efficiency (b_{bp}/b_p) was computed as the ratio of b_{bp} to b_p. Chlorophyll-specific, carbon-specific, and cell-specific optical coefficients were also calculated for particulate absorption, attenuation, and backscattering at 470, 532, and 660 nm. POC values used to estimate carbon-specific coefficients were derived from culture sample measurements, after accounting for dilution in the optical instruments. The Gordon parameter (g), which relates remote-sensing reflectance (R_{rs}) to inherent optical properties (Gordon et al. 1975), was approximated as:

$$g = \frac{b_{bp} + b_{bsw}}{a_p + a_{sw} + b_{bp+}\, b_{bsw}} \quad (6)$$

where a_{sw} and b_{bsw} correspond to pure seawater absorption (Röttgers et al. 2010) and backscattering (Zhang et al. 2009).

Statistical analyses

Nonparametric Spearman correlation coefficients were used to assess relationships between phytoplankton physiological measurements and phytoplankton bio-optical properties at 470, 550, and 660 nm. Correlation coefficients between 0 and 0.39 are described as weak, between 0.4 and 0.59 as moderate, and between 0.6 and 1 as strong. Only significant correlations (p-value ≤ 0.05) are discussed.

Results

Diatom

T. pseudonana doubled every ~ 0.73 d, with cell division beginning during the day, as expected from previous observations (Chisholm et al. 1980) (Fig. 1; Table 1).

It is worth reiterating that in both *T. pseudonana* experiments, cultures were diluted to dawn cell concentrations at each sampling time point after the onset of cell division through dawn when cell division ended. Cell-specific FSC and SSC and red fluorescence increased during daylight and decreased in the dark (Fig. 2).

Minimum values of cell-specific scattering and fluorescence occurred at dawn, but the timing of maximum values varied depending on the property. FSC per cell showed a symmetrical bimodal pattern with maxima at peak irradiance and 2 h after dusk. SSC per cell exhibited a single maximum 2 h before dusk. Red fluorescence per cell displayed an asymmetrical bimodal pattern with maxima at peak irradiance and at the dusk transition. F_v/F_m displayed a symmetrical diel cycle, decreasing from dawn to dusk and then increasing from dusk to dawn (Fig. 3).

A diel pattern was apparent for POC and PON per cell, which increased from dawn to maxima at peak irradiance and again at dusk and then decreased during the night until 4 h before dawn (Fig. 4).

C : N followed similar patterns, but with maxima occurring 2 h before dusk. Chl *a* per cell increased until peak irradiance and then remained relatively constant before decreasing for the first 6 h of night and then increasing until dawn. C : Chl *a* increased in the daylight and decreased in the night.

a_p displayed a symmetrical diel pattern, increasing in the daylight until 4 h before dusk and then decreasing through the night until dawn (Fig. 5).

There was some spectral dependence of a_p, with higher values at 470 nm relative to both 532 and 660 nm. Strong correlations were observed between a_p, c_p, and concentrations of POC, Chl *a*, and cell abundance. a_p was also strongly correlated with concentration-independent properties, including b_{bp}/b_p and proxies for cell size (FSC and SSC per cell and POC per cell), molecular composition (C : N and C : Chl), and pigment activity (red fluorescence per cell and F_v/F_m) (Fig. 6).

Chlorophyll-specific a_p increased for 6 h after dawn, then decreased until dusk and remained constant in the night. Cell-specific a_p showed similar periodicity as a_p, increasing for 6 h after dawn and then decreasing until 4 h before the next dawn (Fig. 7).

The diel periodicity in chlorophyll-specific a_p was particularly pronounced at 470 nm, reflecting the strong absorption properties of Chl *a* and carotenoids at blue wavelengths (Morel and Bricaud 1986). Carbon-specific a_p displayed an opposite trend as chlorophyll-specific and cell-specific a_p,

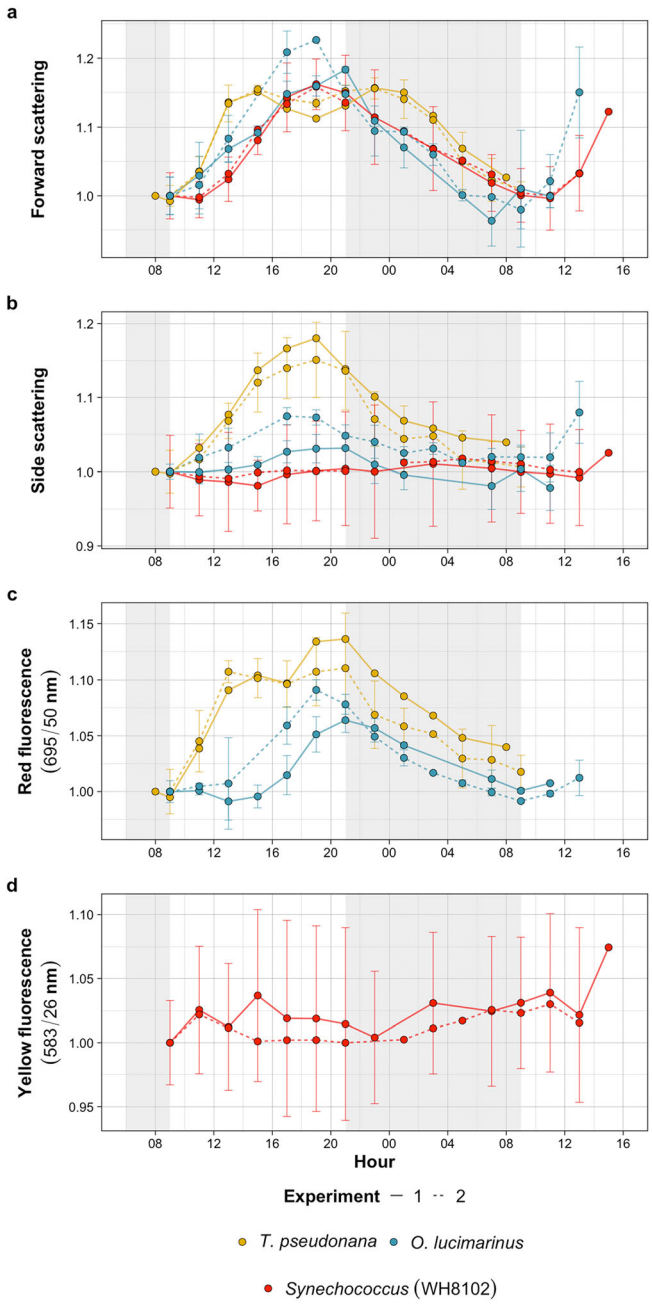

Fig. 2. Cell-specific scattering and fluorescence in the recirculating optical sampling system for each diel experiment. *Thalassiosira pseudonana* and *Ostreococcus lucimarinus* cells were enumerated using red fluorescence (chlorophyll indicator), while *Synechococcus* were enumerated using yellow fluorescence (phycoerythrin indicator). Red fluorescence data for *Synechococcus* are not shown as the flow cytometry settings for the red channel were set too low to resolve cell fluorescence from noise. Values represent population means normalized to the initial condition, with error bars representing the standard deviation.

decreasing from dawn until peak irradiance and then remaining relatively constant before increasing 4 h after dusk (Fig. 7). Spectral variability in the range of each biomass-specific a_p coefficient was greater than the temporal variability (Fig. 8).

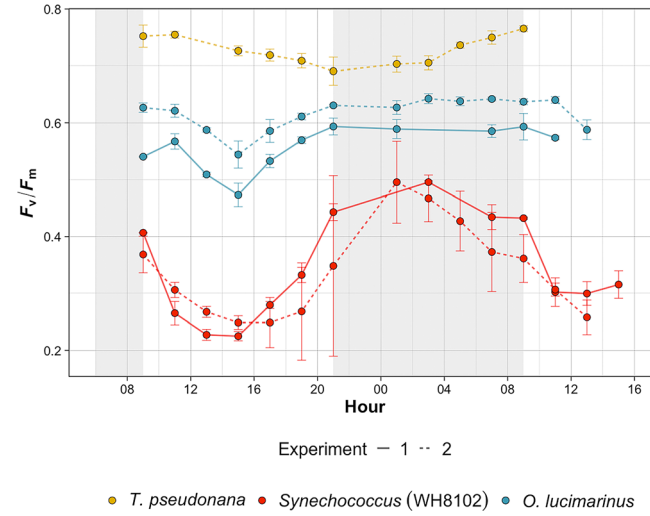

Fig. 3. Variable to maximum fluorescence (F_v/F_m) of cells in cultures for each diel experiment.

c_p showed a similar diel pattern as a_p, but with more asymmetry and little wavelength dependence (Fig. 5). c_p exhibited a weaker correlation with chlorophyll concentrations than a_p, but a stronger correlation with POC concentrations. c_p was similarly correlated to phytoplankton physiological properties as a_p, but showed stronger correlations with concentration-independent properties, including proxies for cell size (FSC per cell, SSC per cell, and POC per cell) and molecular composition (C : N and C : Chl *a*). c_p was also moderately to strongly correlated with pigment activity (red fluorescence per cell and F_v/F_m) and b_{bp}/b_p (Fig. 6). Chlorophyll-specific and cell-specific c_p increased in the daylight and then decreased at night, a pattern opposite that of carbon-specific c_p (Fig. 7). Temporal variability in the range of each biomass-specific c_p coefficient was greater than the spectral variability (Fig. 8).

b_{bp} showed a bimodal pattern over 24 h, with an overall decreasing trend that precluded any significant relationships between b_{bp} and measured metrics of phytoplankton physiology (Figs. 5, 6). b_{bp} did increase from 13 : 00 and 17 : 00 on the 1st day, consistent with previously described daytime increases in b_{bp} (Poulin et al. 2018). Indeed, b_{bp} and c_p were strongly correlated from 13 : 00 on the 1st day to 09 : 00 on the following day ($r \geq 0.81$, $p < 0.01$ for 470, 532, and 660 nm), supporting the link between phytoplankton and diel b_{bp} cycles. The basis of the discrepancy between b_{bp} and c_p between 09 : 00 and 11 : 00 on the 1st day remains unclear. Chlorophyll-specific b_{bp} and cell-specific b_{bp} were also spectrally independent and decreased over the course of the experiment (Fig. 7). Comparatively, carbon-specific b_{bp} followed a pattern akin to that of carbon-specific a_p and c_p, albeit with greater symmetrical periodicity. Like c_p, each biomass-specific b_{bp} coefficient showed greater temporal variability than spectral variability (Fig. 8).

Backscattering efficiency (b_{bp}/b_p), a concentration-independent proxy for cell size and intracellular composition, displayed

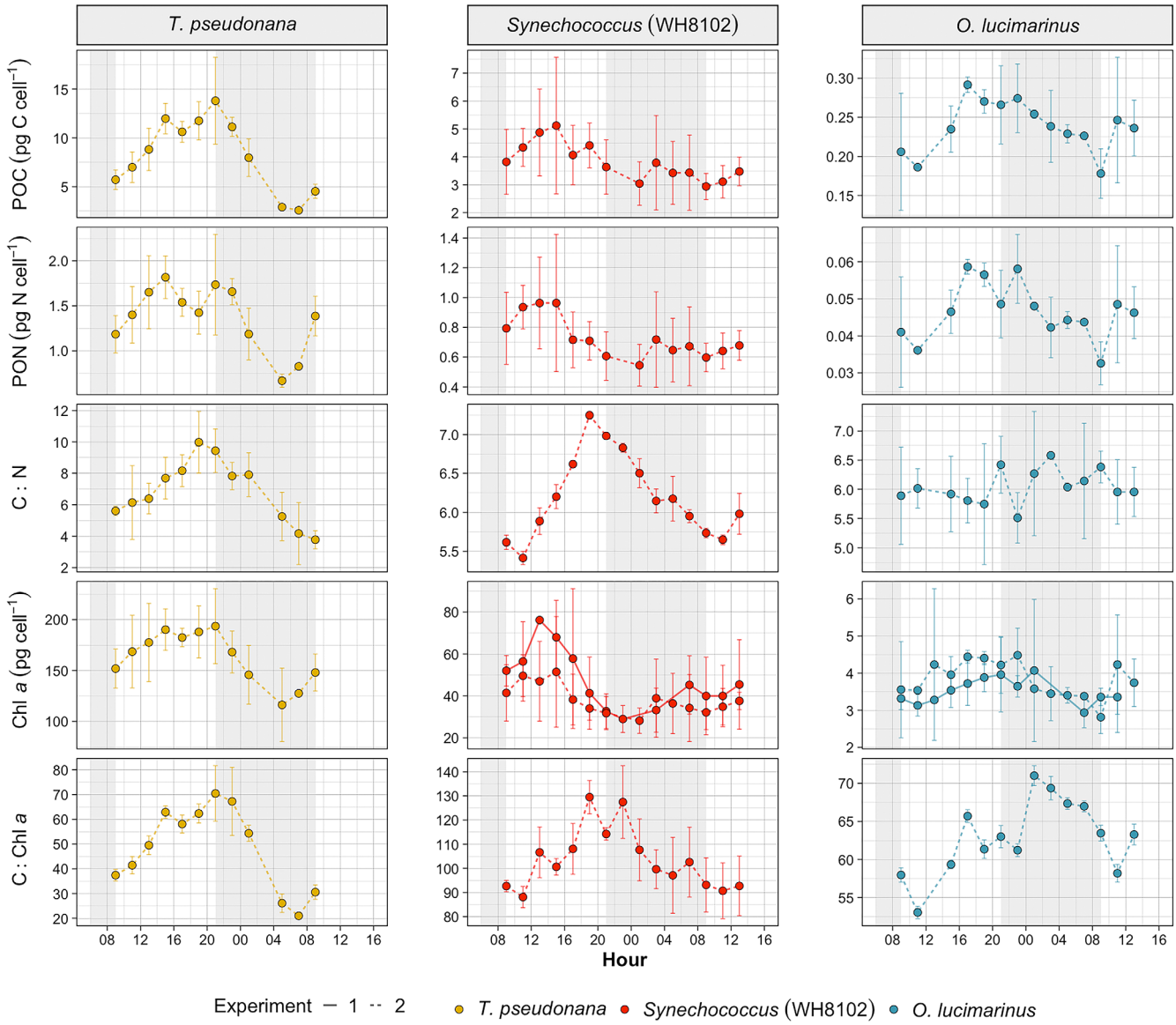

Fig. 4. Carbon, nitrogen, and Chl *a* per cell, as well as carbon to nitrogen (C : N) and carbon to Chl *a* (C : Chl *a*) ratios, estimated for the recirculating optical sampling system for each diel experiment. Values represent means with error bars as standard deviations.

an asymmetric diel pattern without spectral dependence (Fig. 5). b_{bp}/b_p decreased between dawn and 4 h before dusk and it then remained relatively constant for the following 8 h before increasing during the night. Moderate to strong correlations were observed between b_{bp}/b_p and a_p, c_p, as well as concentration-independent proxies for cell size (FSC and SSC per cell and POC per cell), molecular composition (C : N and C : Chl *a*), and pigment activity (red fluorescence per cell and F_v/F_m) (Fig. 6).

Cyanobacterium

Synechococcus doubling time was ~ 3.2 d, with cell division beginning near peak irradiance and ending at the light–dark transition, as previously reported (Waterbury 1986; Armbrust et al. 1989) (Fig. 1; Table 1). In both experiments, FSC per cell increased during the day and decreased in the night, with a maximum 2 h before dusk and minimum at dawn (Fig. 2). SSC per cell and yellow fluorescence per cell were relatively invariant over the day–night cycle. F_v/F_m displayed a diel pattern that varied inversely with irradiance and exhibited a maximum 4 to 6 h after dusk (Fig. 3).

POC and PON per cell were constrained between 3–5 pg C per cell and 0.5–1 pg N per cell, yet still showed a diel pattern of increasing until peak irradiance, decreasing to dusk, and then remaining relatively constant at night (Fig. 4). The C : N diel cycle increased from dawn to 2 h before dusk and then decreased at night. Chlorophyll per cell was higher for the 1st experiment relative to the 2nd, but in both experiments decreased from near peak irradiance until dusk and then

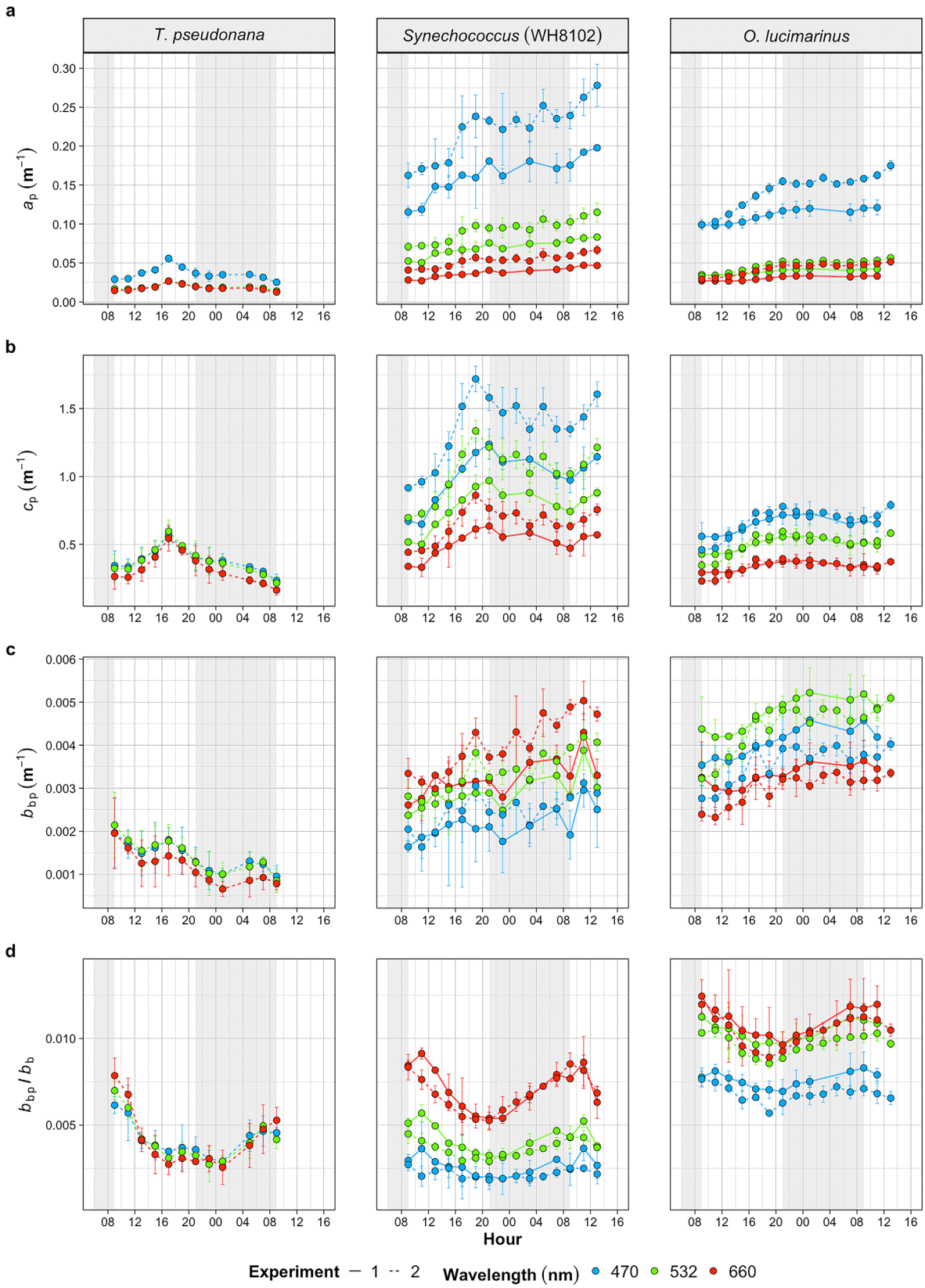

Fig. 5. Temporal changes over the day–night cycle of phytoplankton bio-optical coefficients at 470, 532, and 660 nm, including absorption (a_p), attenuation (c_p), backscattering (b_{bp}) as well as backscattering efficiency (b_{bp}/b_p). Error bars represent standard deviations from mean values.

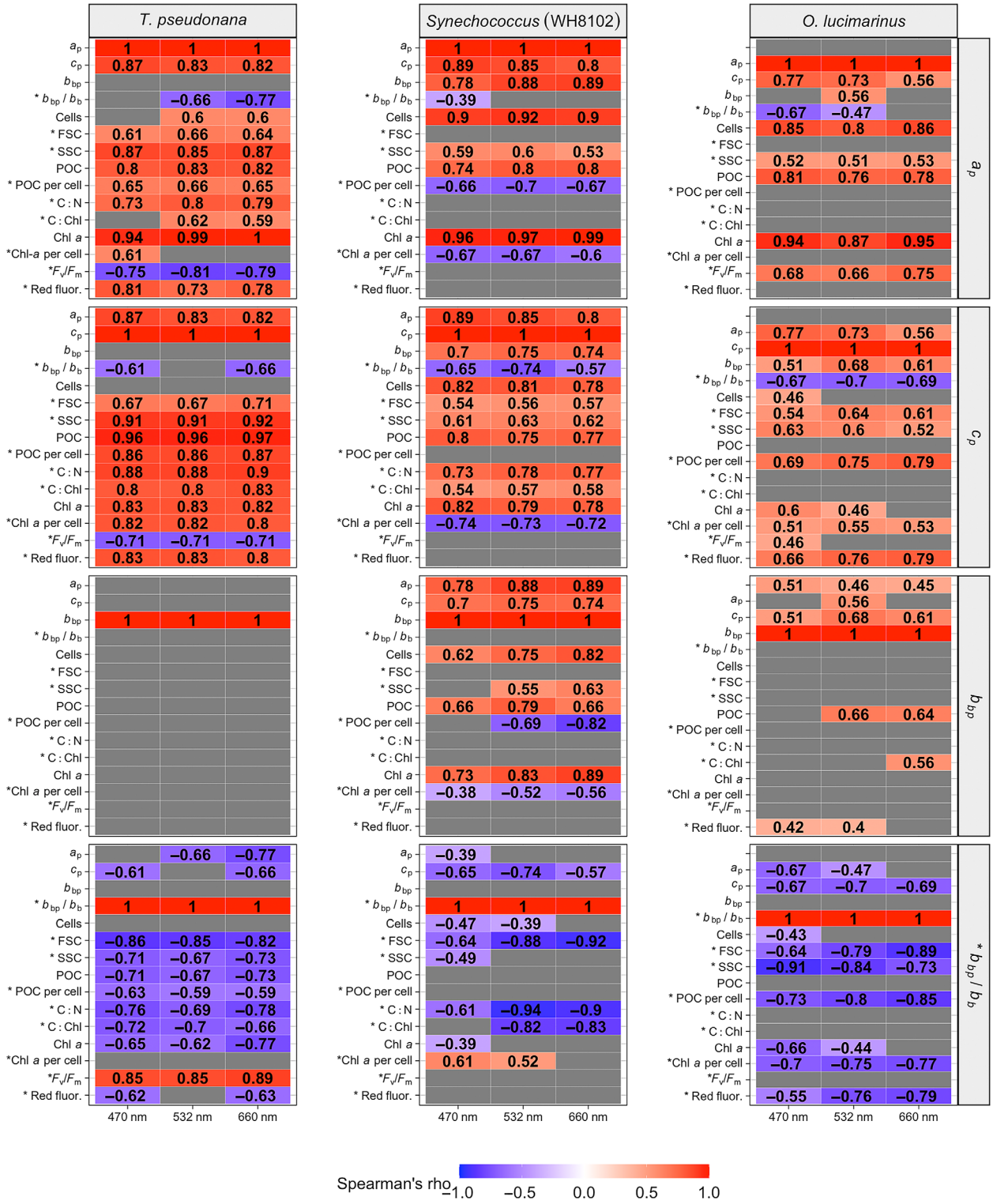

Fig. 6. Nonparametric Spearman correlation coefficients for each phytoplankton (columns) between their physiological properties (*y*-axis for each subplot) and their bio-optical properties (rows) at 470, 532, and 660 nm (*x*-axis for each subplot). Red colors indicate positive correlations while blue colors indicate negative correlations. Variables include absorption (a_p), attenuation (c_p), backscattering (b_{bp}), cell concentrations (cells), total and cellular organic carbon concentrations (POC), total and cellular Chl *a* concentrations, backscattering efficiency (b_{bp}/b_p), FSC per cell, SSC per cell, POC per cell, carbon to nitrogen (C : N), Chl *a* per cell, variable to maximum fluorescence (F_v/F_m), and red fluorescence per cell. Variables with and without an asterisk symbol are concentration independent and concentration dependent, respectively. Only significant correlations (*p*-value ≤ 0.05) are presented.

remained relatively constant throughout the night. C : Chl *a* exhibited a similar diel cycle as C : N.

A diel pattern was absent for a_p, which generally increased from the beginning to the end of each experiment (Fig. 5). Moderate to strong correlations were observed for a_p with c_p, b_{bp}, POC, Chl *a*, and cell concentrations, as well as concentration-independent properties of POC per cell, SSC per cell, and chlorophyll per cell (Fig. 6). Chlorophyll-specific and cell-specific a_p only varied over a small range (as in Stramski et al. 1995) and showed similar wavelength dependencies as a_p. However, some diel periodicity was apparent at 470 and 532 nm corresponding to the absorption properties of Chl *a* and carotenoids in the blue wavelengths and phycoerythrin in the green wavelengths (Fig. 7). Between the two *Synechococcus* experiments, a maximum in cell-specific a_p 2 h before peak irradiance was observed in the 1st experiment that was absent in the 2nd. Both experiments showed a decrease in cell-specific a_p from peak irradiance to dusk followed by little change at night. Carbon-specific a_p exhibited a diel pattern at 470, 532, and 660 nm, decreasing from dawn to dusk and then increasing in the night (Fig. 7). Median chlorophyll-specific a_p showed wide spectral variability, being higher at 470 nm than for 532 and 660 nm. Cell- and carbon-specific a_p also showed greater spectral than temporal variability, in which median values at 470 nm were up to fivefold higher than those at 532 and 660 nm (Fig. 8).

c_p showed spectral dependence, being highest at 470 nm and lowest at 660 nm and was positively correlated to changes in cell abundance (Fig. 5). For the 1st experiment, c_p increased from dawn to a maximum at dusk. For the 2nd experiment, c_p increased from dawn to 2 h before dusk. In both experiments, c_p remained relatively constant over the night. c_p was strongly correlated with b_{bp} and concentrations of chlorophyll, POC, and cell concentrations (Fig. 6). c_p was also moderately to strongly correlated with concentration-independent properties, including b_{bp}/b_p, proxies for cell size (FSC and SSC per cell), and molecular composition (C : N, C : Chl *a*, and Chl *a* per cell). Chlorophyll-specific c_p displayed symmetrical diel periodicity for both experiments, increasing from a minimum at dawn to a maximum 2 h before dusk, and then decreasing over the course of the night (Fig. 7). In contrast, cell-specific c_p increased from dawn until a maximum at peak irradiance and then decreased until 2 h after dusk before settling on a relatively constant value for the remainder of the night. Carbon-specific c_p displayed a muted diel cycle with constrained spectral dependence relative to other biomass-specific coefficients. Nevertheless, all biomass-specific c_p coefficients displayed greater spectral than temporal variability, with highest values at 470 nm and lowest values at 660 nm (Fig. 8). b_{bp} displayed spectral dependence opposite that of c_p, with highest values at 660 nm and the lowest values at 470 nm (Fig. 5). b_{bp} was also moderately to strongly correlated with cell abundance, POC concentration, and chlorophyll concentration as well as concentration-independent properties of SSC per cell, and chlorophyll per cell (Fig. 6). Diel variability was absent in chlorophyll-specific b_{bp}, while cell-specific b_{bp} displayed a similar pattern to cell-specific a_p and c_p. Carbon-specific b_{bp} exhibited a temporal pattern similar to carbon-specific a_p and opposite that of carbon-specific c_p (Fig. 7). Biomass-specific b_{bp} coefficients varied spectrally and temporally (Fig. 8).

b_{bp}/b_p exhibited a symmetrical diel pattern of decreasing between dawn and dusk and increasing from dusk to dawn, with absolute values varying with wavelength (Fig. 5). b_{bp}/b_p was correlated with a_p at 532 nm, c_p, cell abundance, and chlorophyll concentrations, as well as concentration-independent physiological metrics for cell size (FSC and SSC per cell), and molecular composition (C : N, C : Chl *a*, and Chl *a* per cell) (Fig. 6).

Picoeukaryote

O. lucimarinus had a doubling time of ~ 1.9 d, dividing predominantly in the dark, as is often the case for eukaryotic phytoplankton (Nelson and Brand 1979). Cell division was minimal in the 1st experiment and more apparent in the 2nd experiment (Fig. 1, Table 1). In both experiments, scattering per cell and red fluorescence per cell displayed diel patterns of daytime increases and nighttime decreases. However, the timing of maximum values for these parameters were offset between the two experiments, peaking at dusk for the 1st experiment and 2 h before dusk for the 2nd experiment (Fig. 2). F_v/F_m displayed a narrow diel cycle for both experiments that varied inversely with irradiance and remained constant at night.

POC and PON per cell were low and constrained between 0.17–0.29 pg C per cell and 0.03–0.06 pg N per cell, showing a diel pattern of daytime increase and nighttime decrease (Fig. 4). C : N exhibited a small range and a muted diel cycle with an increase at the light–dark transition. Chlorophyll per cell was similar between the two experiments, increasing in the day and decreasing at night. C : Chl *a* indicated an accumulation of carbon relative to Chl *a* from the beginning to the end of the experiment and showed a diel pattern of increasing from 2 h after dawn until 4 h after dusk.

a_p was spectrally dependent, with highest values at 470 nm and lowest at 660 nm (Fig. 5). a_p increased over the duration of both experiments, displaying the highest increases of up to a factor of 2 in the 2nd experiment. Strong correlations were observed between a_p, Chl *a* and cell concentrations. a_p was also correlated with concentration-independent properties of C : Chl, SSC per cell, F_v/F_m, and b_{bp}/b_p (Fig. 6). Chlorophyll-specific a_p showed little diel variability, while cell-specific a_p displayed diel periodicity of increasing from dawn to dusk and decreasing from dusk to dawn. Carbon-specific a_p exhibited a low diel variability, decreasing from 2 h after dawn until 4 h after dusk and then increasing into the following morning (Fig. 7). Biomass-specific a_p was spectrally dependent, with highest values at 470 nm and lowest at 532 nm (Fig. 8).

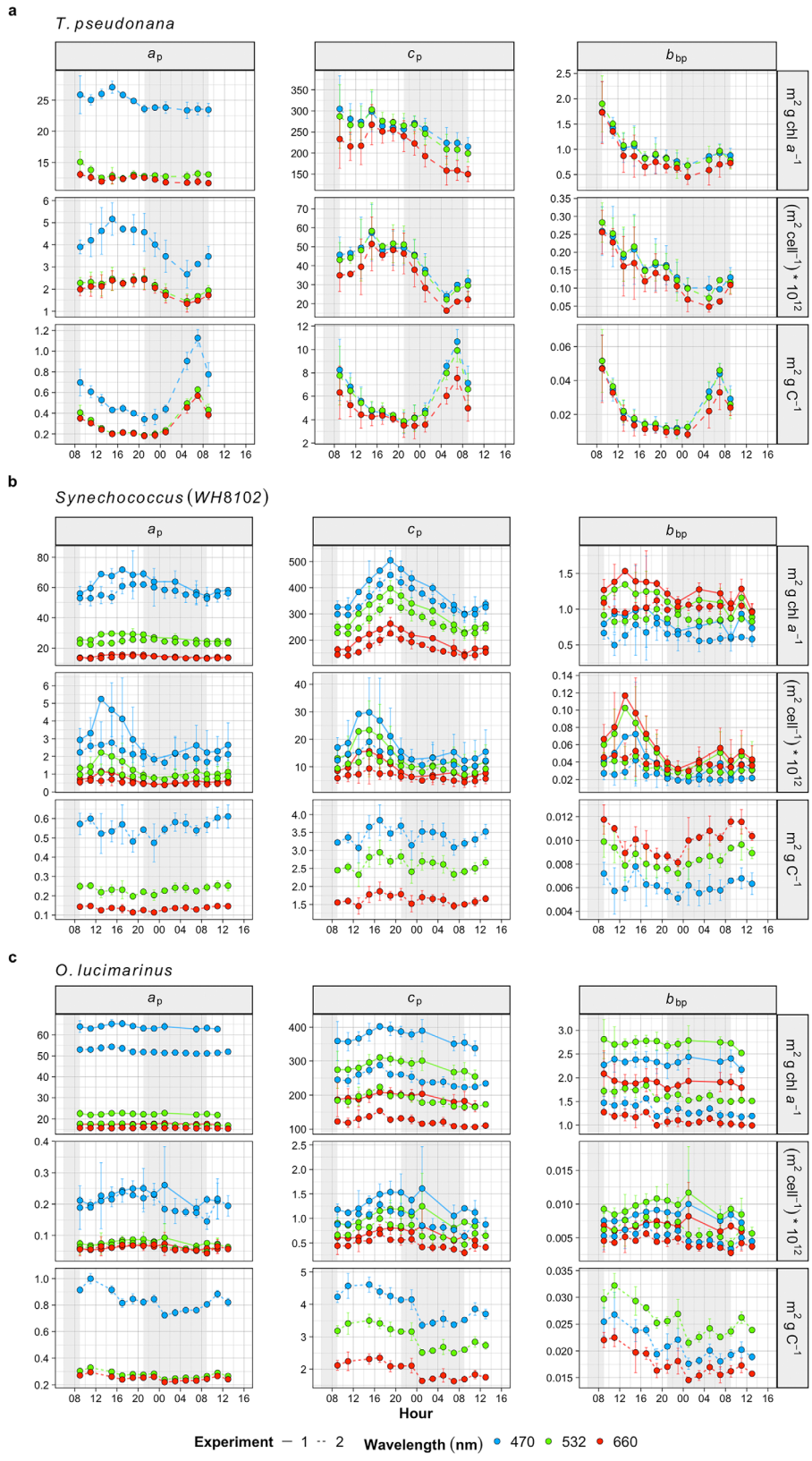

Fig. 7. Biomass-specific bio-optical properties at 470, 532, and 660 nm over the diel cycle for each phytoplankton and each experiment. Bio-optical coefficients include those normalized to Chl *a* concentrations, to cell concentrations, and to particulate organic carbon concentrations. Error bars represent standard deviations from mean values.

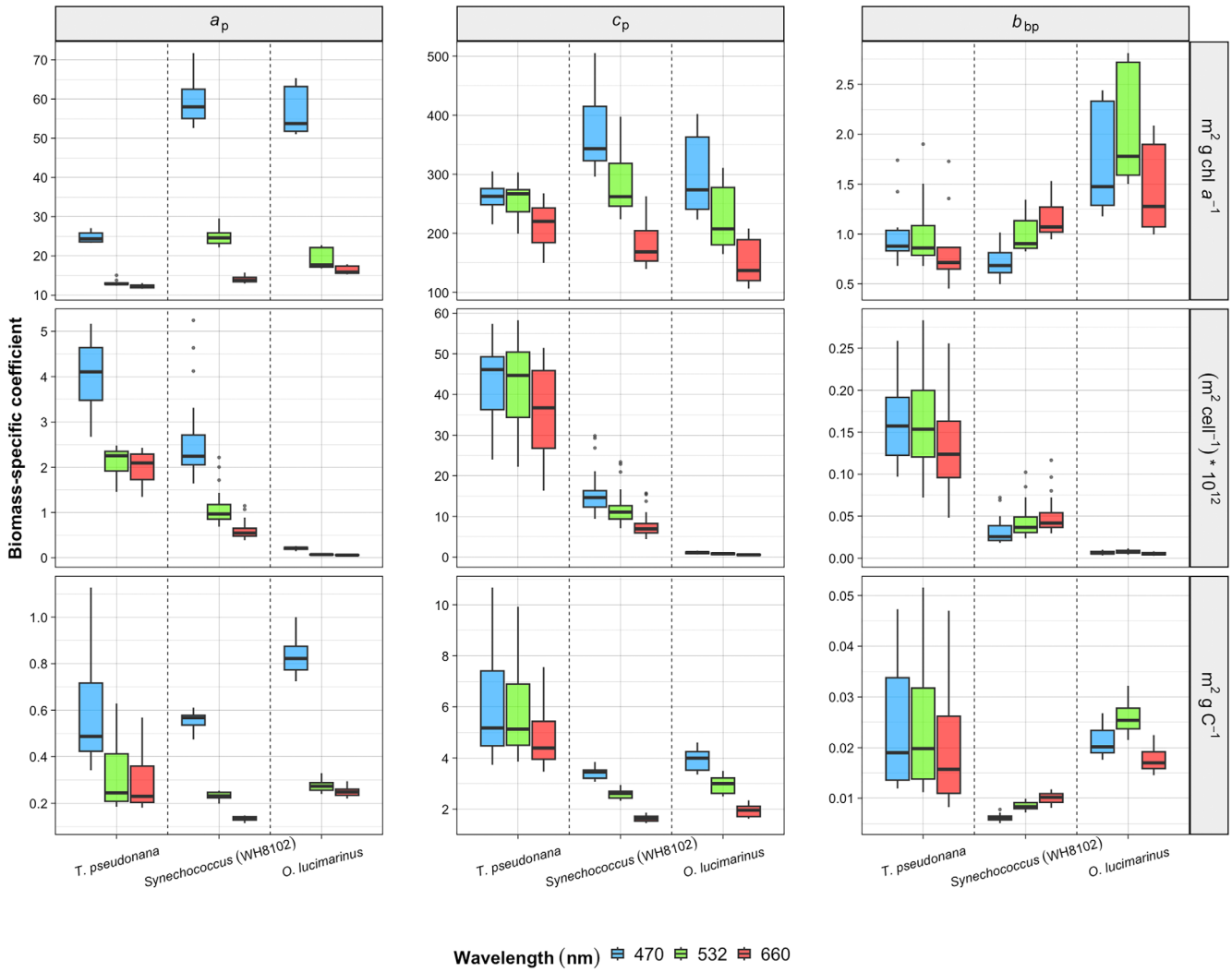

Fig. 8. Box and whisker plots comparing biomass-specific bio-optical properties at 470, 532, and 660 nm between each phytoplankton. Boxes represent the median and the 1st and 3rd quartiles. Whiskers represent the 1.5 interquartile range. Circles indicate outliers.

c_p showed the same spectral dependence as a_p and displayed a diel cycle, increasing from dawn to dusk and decreasing from dusk to dawn (Fig. 5). The range in c_p was similar between both experiments. c_p exhibited a weaker correlation with cell abundance and chlorophyll concentration than a_p. c_p was correlated with b_{bp} as well as with concentration-independent properties of b_{bp}/b_p, cell size (FSC and SSC per cell and POC per cell), and pigment activity (red fluorescence per cell and F_v/F_m) (Fig. 6). Both chlorophyll- and cell-specific c_p showed the same symmetrical diel periodicity as c_p. Carbon-specific c_p displayed a stepwise decrease 4 h after dusk (Fig. 7). Each biomass-specific c_p coefficient displayed greater spectral than temporal variability (Fig. 8).

b_{bp} displayed a spectral dependence that differed from that of a_p and c_p, with the highest values at 532 nm and the lowest at 660 nm (Fig. 5). b_{bp} was not correlated with cell abundance but was correlated with POC concentrations and concentration-independent properties of C : Chl and red fluorescence per cell (Fig. 6). Chlorophyll- and cell-specific b_{bp} did not show clear diel patterns. Carbon-specific b_{bp} exhibited a similar diel pattern to carbon-specific c_p (Fig. 7). Biomass-specific b_{bp} coefficients displayed less spectral variability than a_p or c_p (Fig. 8).

b_{bp}/b_p exhibited a symmetrical diel pattern and its magnitude depended on wavelength. b_{bp}/b_p decreased between dawn and dusk and then increased from dusk to dawn for both experiments (Fig. 5). b_{bp}/b_p was correlated with a_p, c_p, cell abundance, chlorophyll concentrations, as well as concentration-independent proxies for cell size (FSC and SSC per cell, POC per cell), chlorophyll per cell, and red fluorescence per cell (Fig. 6).

Discussion

Bio-optical properties are thought to vary to first order with particle concentration and thus could be expected to follow

cell division patterns. Each of the studied phytoplankton exhibited synchronized cell division coupled to the light–dark cycle, but they differed in timing and duration (Fig. 1). Diel changes in a_p were linked to changes in cell concentration for all three species, but associations between changes in c_p and b_{bp} with cell concentration were generally restricted to *Synechococcus* (Fig. 8). Changes in c_p and b_{bp} over the diel cycle may thus be more sensitive to physiological properties, including cell size and refractive index, that change more continuously than more stepwise increases in cell concentrations (Stramski and Reynolds 1993; Stramski et al. 1995; DuRand and Olson 1998; DuRand et al. 2002). The suite and strength of correlations between each bio-optical property and metrics of cell physiology varied spectrally and by species (Fig. 8). Despite interspecific differences in timing and magnitude, diel cycles in physiological properties and bio-optical properties are often likely to correspond to photoacclimation, daytime accumulation of energy and carbon, and nighttime metabolism and respiration (Figs. 4, 8).

Changes in cell physiology attuned to the day–night cycle

The phytoplankton studied here all showed diel changes in chlorophyll per cell, pigment absorption ratios, F_v/F_m and fluorescence per cell that corresponded to changes in light intensity. Photophysiological responses to both excess and low light were evidenced by changes in pigmentation, particularly ratios of photoprotective carotenoids and accessory pigments to Chl *a* (Supporting Information Fig. S2), F_v/F_m minima at peak irradiance for *Synechococcus* and *O. lucimarinus* (Fig. 3.), and daytime increases and nighttime decreases in red fluorescence per cell for *T. pseudonana* and *O. lucimarinus* (Fig. 4).

Phytoplankton diel periodicity in cell size and intracellular composition were strongly associated with changes in cellular optical properties that alter the bulk properties of seawater. In all species, daytime increases in cell size due to carbon accumulation from photosynthesis were reversed by cell division and respiration (Fig. 4). These behaviors were captured by diel changes in cell-specific forward light scattering and c_p in all species (consistent with Olson et al. 1989; Olson et al. 1990; DuRand et al. 2002) as well as similar changes in cell-specific SSC in the eukaryotic cells (Figs. 1, 2). This is consistent with previous observations for picoeukaryotes in which diel changes in cell-specific SSC corresponded to changes in cell size (Simon et al. 1994; Vaulot and Marie 1999). b_{bp}/b_p has been suggested as a sensitive proxy for the bulk refractive index of natural particle assemblages (Ulloa et al. 1994; Twardowski et al. 2001; Boss et al. 2004), and it has been observed to increase with decreasing cell size in different phytoplankton taxa (Vaillancourt et al. 2004; Whitmire et al. 2010). For all three phytoplankton studied here, diel changes in b_{bp}/b_p reflected cell growth and division and/or respiration (Figs. 4, 5). In addition, C : N ratios for each phytoplankton showed the expected diel pattern in which carbon-rich compounds (e.g., carbohydrates) accumulate faster than nitrogen-rich compounds (e.g., proteins) during the day, which is then reversed at night due to protein synthesis and respiration (Halsey and Jones 2015) (Fig. 4).

Sensitivity of absorption, attenuation, and backscattering to diel changes in physiology

a_p is primarily impacted by cell concentration, composition, and concentration of intracellular pigments, the efficiency of absorption by those pigments, and cell size (Morel and Bricaud 1981; Bricaud et al. 1983). Ahn et al. (1992) noted that variations in chlorophyll-specific a_p are the product of interspecific differences in cell size and intracellular pigment concentrations. Thus, both interspecific differences and diel patterns in biomass-specific a_p observed in this study likely reflect changes in pigmentation (concentration and composition) and cell size (Fig. 7). Larger cells and cells with higher internal concentrations of pigments have been hypothesized to exhibit a strong "package effect," that is, decreased absorption per unit of pigment (Morel and Bricaud 1981). This could be supported by this study with *T. pseudonana* exhibiting lower chlorophyll-specific a_p than *Synechococcus* and *O. lucimarinus*. Furthermore, the relatively invariant chlorophyll-specific a_p at 660 nm for *Synechococcus* and 470, 532, and 660 nm for *O. lucimarinus* may reflect a minimal contribution of a "package effect" at these wavelengths for these species. As *T. pseudonana* and *Synechococcus* cells increase in size (e.g., FSC per cell or POC per cell), chlorophyll-specific a_p increases. The corresponding increases in cell size and chlorophyll-specific a_p for these species is contrary to the prediction of a "package effect" and may be attributed to coincident increases in intracellular carotenoid concentrations, highlighting the complexity of the relationship between phytoplankton physiology and light. Furthermore, cell-specific a_p for *T. pseudonana*, *Synechococcus*, and *O. lucimarinus* increased during periods of cell expansion. (Fig. 7). *T. pseudonana* exhibited diel variability in the Gordon parameter (g) at 470 nm, with decreases in the day due to increasing cell size and pigment absorption and increases at night due to division (Supporting Information Fig. S3). Comparatively, g did not show diel variability at 532 and 660 nm for *T. pseudonana* nor at 470, 532, and 660 nm for either *Synechococcus* or *O. lucimarinus*. These results suggest that changes in reflectance in regions of chlorophyll absorption are more impacted by diel cycles of species like *T. pseudonana* than species like *Synechococcus and O. lucimarinus*.

c_p is the sum of a_p and b_p and is thus impacted by pigmentation, cell size, and refractive index (Kirk 1975; Jerlov 1976). c_p was dominated by scattering processes and consequently, was likely more sensitive to changes in cell size and refractive index than to changes in pigmentation as the average contribution of a_p to c_p was 5–19% for the phytoplankton species studied here. c_p can increase with cell concentration if cell size remains constant or with cell size if cell concentration remains constant (Kirk 1975). *T. pseudonana* followed these expectations, showing inverse patterns between

cell- and carbon-specific c_p, with cell-specific c_p increasing with cell size in the day prior to division and carbon-specific c_p increasing following division at night (Figs. 4, 7). Diel changes up to 2.75-fold in the carbon-specific c_p coefficient contrast with previous observations of relatively constant carbon-specific c_p over the day–night cycle for *T. pseudonana* (Stramski and Reynolds 1993). *Synechococcus* and *O. lucimarinus* also showed increases and decreases in cell-specific c_p corresponding to increases and decreases in cell size. *Synechococcus*, however, showed little to no change in cell-specific c_p or carbon-specific c_p during the night when division was arrested and changes in POC, POC per cell, and Chl *a* per cell were minimal (Figs. 4 and 7).While c_p and b_{bp} can be well correlated across their full dynamic ranges in the ocean (Dall'Olmo et al. 2009; Westberry et al. 2010), they can also be decoupled in timing and amplitude over the diel cycle (Loisel et al. 2011; Kheireddine and Antoine 2014; Poulin et al. 2018). In the current study, c_p and b_{bp} followed strongly correlated temporal patterns in *Synechococcus* and *O. lucimarinus*, but c_p showed amplitude changes ~ twofold higher than b_{bp} across all species (Fig. 5). For *Synechococcus* and *O. lucimarinus*, c_p correlated with each physiological metric covarying with b_{bp}, but c_p also showed correlations with other physiological metrics not covarying with b_{bp} (Fig. 6). These relationships may help to explain the temporal variability of biomass-specific c_p and b_{bp}. For example, opposite patterns between carbon-specific b_{bp} and c_p were exhibited in *Synechococcus*. Changes in carbon-specific c_p for *Synechococcus* intuitively follow changes in cell size. By contrast, the decreasing carbon-specific b_{bp} during the day may reflect the lower backscattering efficiency (b_{bp}/b_b) of expanding cells while the increasing carbon-specific b_{bp} in the night may reflect the higher b_{bp}/b_b of cells that lose volume from division and respiration (Figs. 5, 7).

Comparison of normalized bio-optical coefficients with previous studies

Field and modeling studies often assume constant carbon-specific attenuation coefficients (Siegel et al. 1989; Stramska and Dickey 1992) or chlorophyll-specific absorption coefficients (Morel 1991) over the day–night cycle when converting optical measurements into POC concentrations and primary production rates. In this study, interspecific variability in normalized bio-optical coefficients decreased when the dynamic range of the properties they were normalized to also decreased. Specifically, variability was highest when bio-optical coefficients were normalized to cell concentration, less when normalized to Chl *a*, and the least when normalized to carbon (consistent with observations by Stramski and Reynolds 1993; Vaillancourt et al. 2004) (Fig. 8). Thus, POC concentrations and primary production rates can be derived from in situ and remote optical measurements using constant carbon-specific bio-optical coefficients, but caution should be exercised before making the same derivations using constant cell- or chlorophyll-specific bio-optical coefficients.

Interspecific variability for each bio-optical coefficient was greater than diel variability for a single species, in agreement with previous studies (DuRand et al. 2002; Poulin et al. 2018). Across all three species over the diel cycle, the median chlorophyll-specific c_p coefficient at 660 nm (169 ± 48 m^2 g Chl a^{-1}) fell within the range reported over various areas of the open ocean (40–1420 m^2 g Chl a^{-1}) (Behrenfeld and Boss 2003), while the median chlorophyll-specific b_{bp} coefficient at 532 nm (1.2 ± 0.5 m^2 g Chl a^{-1}) fell at the low end of the range reported for 9 cultured phytoplankton species by Ahn et al. (1992) (0.023–9.9 m^2 g Chl a^{-1} at 550 nm) and 13 different species by Whitmire et al. (2010) (0.3–463 m^2 g Chl a^{-1} at 550 nm). Cell-specific and carbon-specific b_{bp} for all species showed a similar range to those reported by Poulin et al. (2018). At 660 nm, *T. pseudonana* showed the highest cell-specific c_p coefficients, with values similar to previous studies (Stramski et al. 1995; Poulin et al. 2018). By contrast, cell-specific c_p values for *Synechococcus* were ~ 4 times lower than *T. pseudonana*, yet still ~ 10 times higher values than values previously reported for another *Synechococcus* strain (WH8103) (Stramski et al. 1995). *O. lucimarinus* had cell-specific c_p values a factor of ~ 55 lower than *T. pseudonana*. Similarly, carbon-specific c_p values were highest for *T. pseudonana* and lowest for *O. lucimarinus*, with the overall mean value at 660 nm (2.7 ± 1.6 m^2 g C^{-1}) being comparable to those reported by previous diel studies including for *T. pseudonana* (3.81 m^2 g C^{-1}) (Stramski and Reynolds 1993), *Synechococcus* (2.48 m^2 g C^{-1}) (Stramski et al. 1995), *Nannochloris* (3–4 m^2 g C^{-1}) (DuRand and Olson 1998), and *M. pusilla* (2.5–3.8 m^2 g C^{-1}) (DuRand et al. 2002).

Conclusion

Variations in phytoplankton bio-optical properties are intertwined with diel changes in cell morphology, composition, and photophysiology. The current study provides the first culture-based characterization of complete diel cycles in b_{bp} and, for the three species examined here, observed day–night changes ranged between 1.2- and 3-fold. Time of day is thus an important factor to consider when interpreting satellite-retrieved data. Diel changes in many bio-optical properties also differed in timing and magnitude between species, emphasizing the additional importance of phytoplankton community composition in interpreting remotely detected optical properties.

Data availability statement

All generated data, analyses, and code used for this study are publicly available on GitHub (https://github.com/nbaetge/diel_optics_phyto_cultures) and through the OSU Ocean Productivity Website (https://sites.science.oregonstate.edu/ocean.productivity/).

References

Ahn, Y.-H., A. Bricaud, and A. Morel. 1992. Light backscattering efficiency and related properties of some phytoplankters. Deep Sea Res. A Oceanogr. Res. Pap. **39**: 1835–1855. doi:10.1016/0198-0149(92)90002-B

Armbrust, E. V., J. D. Bowen, R. J. Olson, and S. W. Chisholm. 1989. Effect of light on the cell cycle of a marine *Synechococcus* strain. Appl. Environ. Microbiol. **55**: 425–432. doi:10.1128/aem.55.2.425-432.1989

Becker, K. W., and others. 2018. Daily changes in phytoplankton lipidomes reveal mechanisms of energy storage in the open ocean. Nat. Commun. **9**: 5179. doi:10.1038/s41467-018-07346-z

Behrenfeld, M. J., and E. Boss. 2003. The beam attenuation to chlorophyll ratio: An optical index of phytoplankton physiology in the surface ocean? Deep Sea Res. I Oceanogr. Res. Pap. **50**: 1537–1549. doi:10.1016/j.dsr.2003.09.002

Behrenfeld, M. J., E. Boss, D. A. Siegel, and D. M. Shea. 2005. Carbon-based ocean productivity and phytoplankton physiology from space. Global Biogeochem. Cycl. **19**: 1–14. doi:10.1029/2004GB002299

Behrenfeld, M. J., and others. 2019. Global satellite-observed daily vertical migrations from ocean animals. Nature **576**: 257–263. doi:10.1038/s41586-0191796-9

Bolaños, L. M., and others. 2020. Small phytoplankton dominate western North Atlantic biomass. ISME J. **14**: 1663–1674. doi:10.1038/s41396-020-0636-0

Boss, E., W. S. Pegau, M. Lee, M. Twardowski, E. Shybanov, G. Korotaev, and F. Baratange. 2004. Particulate backscattering ratio at LEO 15 and its use to study particle composition and distribution. J. Geophys. Res. Oceans **109**: 1–10. doi:10.1029/2002jc001514

Boss, E. S., R. Collier, G. Larson, K. Fennel, and W. S. Pegau. 2007. Measurements of spectral optical properties and their relation to biogeochemical variables and processes in Crater Lake, Crater Lake National Park, OR. Hydrobiologia **574**: 149–159. doi:10.1007/s10750-006-2609-3

Brand, L. E. 1982. Persistent diel rhythms in the chlorophyll fluorescence of marine phytoplankton species. Mar. Biol. **69**: 253–262. doi:10.1007/BF00397491

Bricaud, A., A. Morel, and L. Prieur. 1983. Optical efficiency factors of some phytoplankters. Limnol. Oceanogr. **28**: 816–832. doi:10.4319/lo.1983.28.5.0816

Brown, M., W. B. Penta, B. Jones, and M. Behrenfeld. 2019. The ratio of single-turnover to multiple-turnover fluorescence varies predictably with growth rate and cellular chlorophyll in the green alga *Dunaliella tertiolecta*. Photosynth. Res. **140**: 65–76. doi:10.1007/s11120-018-00612-7

Chase, A., E. Boss, R. Zaneveld, A. Bricaud, H. Claustre, J. Ras, G. Dall'Olmo, and T. K. Westberry. 2013. Decomposition of in situ particulate absorption spectra. Methods Oceanogr. **7**: 110–124. doi:10.1016/j.mio.2014.02.002

Chisholm, S., F. Morel, and W. Slocum. 1980. The phasing and distribution of cell division cycles in marine diatoms, p. 281–300. *In* P. G. Falkowski [ed.], Primary productivity in the sea. Environmental Science Research, vol 19. Springer. doi:10.1007/978-1-4684-3890-1_16

Claustre, H., A. Bricaud, M. Babin, F. Bruyant, L. Guillou, F. L. Gall, D. Marie, and F. Partensky. 2002. Diel variations in *Prochlorococcus* optical properties. Limnol. Oceanogr. **47**: 1637–1647. doi:10.4319/lo.2002.47.6.1637

Cuhel, R. L., P. B. Ortner, and D. R. S. Lean. 1984. Night synthesis of protein by algae. Limnol. Oceanogr. **29**: 731–744. doi:10.4319/lo.1984.29.4.0731

Dall'Olmo, G., T. K. Westberry, M. J. Behrenfeld, E. Boss, and W. H. Slade. 2009. Significant contribution of large particles to optical backscattering in the open ocean. Biogeosciences **6**: 947–967. doi:10.5194/bg-6-947-2009

Durand, M. D., and R. J. Olson. 1996. Contributions of phytoplankton light scattering and cell concentration changes to diel variations in beam attenuation in the equatorial pacific from flow cytometric measurements of pico-, ultra- and nanoplankton. Deep-Sea Res. II Top. Stud. Oceanogr. **43**: 891–906. doi:10.1016/0967-0645(96)00020-3

DuRand, M. D., and R. J. Olson. 1998. Diel patterns in optical properties of the chlorophyte Nannochloris sp.: Relating individual-cell to bulk measurements. Limnol. Oceanogr. **43**: 1107–1118. doi:10.4319/lo.1998.43.6.1107

DuRand, M. D., R. E. Green, H. M. Sosik, and R. J. Olson. 2002. Diel variations in optical properties of *Micromonas pusilla* (Prasinophyceae). J. Phycol. **38**: 1132–1142. doi:10.1046/j.1529-8817.2002.02008.x

Goldman, C. R., D. T. Mason, and J. E. Hobbie. 1969. Variations in photosynthesis in two shallow Antarctic lakes. SIL Proc. **17**: 414–418. doi:10.1080/03680770.1968.11895866

Gordon, H. R., O. B. Brown, and M. M. Jacobs. 1975. Computed relationships between the inherent and apparent optical properties of a flat homogeneous ocean. Appl. Optics **14**: 417–427. doi:10.1364/AO.14.000417

Guillard, R. R. L., and J. H. Ryther. 1962. Studies of marine planktonic diatoms. I. *Cyclotella nana* Hustedt and *Detonula confervacea* Cleve. Can. J. Microbiol. **8**: 229–239. doi:10.1139/m62-029

Guillard, R. R. L., and P. E. Hargraves. 1993. *Stichochrysis immobilis* is a diatom, not a chrysophyte. Phycologia **32**: 234–236. doi:10.2216/i0031-8884-32-3-234.1

Haëntjens, N., and E. Boss. 2020. Inlinino: A modular software data logger for oceanography. Oceanography **33**: 80–84. doi:10.5670/oceanog.2020.112

Halsey, K., A. Milligan, and M. Behrenfeld. 2014. Contrasting strategies of photosynthetic energy utilization drive lifestyle strategies in ecologically important picoeukaryotes. Metabolites **4**: 260–280. doi:10.3390/metabo4020260

Halsey, K. H., and B. M. Jones. 2015. Phytoplankton strategies for photosynthetic energy allocation. Ann. Rev. Mar. Sci. **7**: 265–297. doi:10.1146/annurev-marine-010814-015813

Harding, L. W., B. W. Meeson, B. B. Prézelin, and B. M. Sweeney. 1981. Diel periodicity of photosynthesis in marine phytoplankton. Mar. Biol. **61**: 95–105. doi:10.1007/BF00386649

Herman, E. M., and B. M. Sweeney. 1975. Circadian rhythm of chloroplast ultrastructure in *Gonyaulax polyedra*, concentric organization around a central cluster of ribosomes. J. Ultrastruct. Res. **50**: 347–354. doi:10.1016/S0022-5320(75)80065-7

Jacquet, S., F. Partensky, J.-F. Lennon, and D. Vaulot. 2001. Diel patterns of growth and division in marine picoplankton in culture. J. Phycol. **37**: 357–369.

Jerlov, N. G. 1976. Marine optics. Elsevier.

Kheireddine, M., and D. Antoine. 2014. Diel variability of the beam attenuation and backscattering coefficients in the northwestern Mediterranean Sea (BOUSSOLE site). J. Geophys. Res. Ocean. **119**: 5465–5482. doi:10.1002/2014JC010007

Kirk, J. T. O. 1975. A theoretical analysis of the contribution of algal cells to the attenuation of light within natural waters II. Spherical cells. New Phytol. **75**: 21–36. doi:10.1111/j.1469-8137.1975.tb01367.x

Kolber, Z. S., O. Prášil, and P. G. Falkowski. 1998. Measurements of variable chlorophyll fluorescence using fast repetition rate techniques: Defining methodology and experimental protocols. Biochim. Biophys. Acta Bioenerg. **1367**: 88–106. doi:10.1016/S0005-2728(98)00135-2

Kostakis, I., M. Twardowski, C. Roesler, R. Röttgers, D. Stramski, D. McKee, A. Tonizzo, and S. Drapeau. 2021. Hyperspectral optical absorption closure experiment in complex coastal waters. Limnol. Oceanogr. Methods **19**: 589–625. doi:10.1002/lom3.10447

Loisel, H., and others. 2011. Characterization of the bio-optical anomaly and diurnal variability of particulate matter, as seen from scattering and backscattering coefficients, in ultra-oligotrophic eddies of the Mediterranean Sea. Biogeosciences **8**: 3295–3317. doi:10.5194/bg-8-3295-2011

Mackey, K. R. M., A. Paytan, K. Caldeira, A. R. Grossman, D. Moran, M. McIlvin, and M. A. Saito. 2013. Effect of temperature on photosynthesis and growth in marine *Synechococcus* spp. Plant Physiol. **163**: 815–829.

Maxwell, K., and G. N. Johnson. 2000. Chlorophyll fluorescence—A practical guide. J. Exp. Bot. **51**: 659–668. doi:10.1093/jexbot/51.345.659

Milligan, A. J., U. A. Aparicio, and M. J. Behrenfeld. 2012. Fluorescence and nonphotochemical quenching responses to simulated vertical mixing in the marine diatom *Thalassiosira weissflogii*. Mar. Ecol. Prog. Ser. **448**: 67–78. doi:10.3354/meps09544

Morel, A. 1991. Light and marine photosynthesis: A spectral model with geochemical and climatological implications. Prog. Oceanogr. **26**: 263–306. doi:10.1016/0079-6611(91)90004-6

Morel, A., and A. Bricaud. 1981. Theoretical results concerning light absorption in a discrete medium, and application to specific absorption of phytoplankton. Deep Sea Res. A Oceanogr. Res. Pap. **28**: 1375–1393. doi:10.1016/0198-0149(81)90039-X

Morel, A., and A. Bricaud. 1986. Inherent optical properties of algal cells including picoplankton: Theoretical and experimental results. Can. Bull. Fish. Aquat. Sci. **214**: 521–559.

Morel, A., and L. Prieur. 1977. Analysis of variations in ocean color. Limnol. Oceanogr. **22**: 709–722. doi:10.4319/lo.1977.22.4.0709

Morel, F. M. M., R. J. M. Hudson, and N. M. Price. 1991. Limitation of productivity by trace metals in the sea. Limnol. Oceanogr. **36**: 1742–1755. doi:10.4319/lo.1991.36.8.1742

Nelson, D. M., and L. E. Brand. 1979. Cell division periodicity in 13 species of marine phytoplankton on a light: Dark cycle. J. Phycol. **15**: 67–75. doi:10.1111/j.1529-8817.1979.tb02964.x

Olson, R. J., E. R. Zettler, and O. K. Anderson. 1989. Discrimination of eukaryotic phytoplankton cell types from light scatter and autofluorescence properties measured by flow cytometry. Cytometry **10**: 636–643. doi:10.1002/cyto.990100520

Olson, R. J., S. W. Chisholm, E. R. Zettler, and E. V. Armbrust. 1990. Pigments, size, and distributions of *Synechococcus* in the North Atlantic and Pacific Oceans. Limnol. Oceanogr. **35**: 45–58. doi:10.4319/lo.1990.35.1.0045

Owens, T. G., P. G. Falkowski, and T. E. Whitledge. 1980. Diel periodicity in cellular chlorophyll content in marine diatoms. Mar. Biol. **59**: 71–77. doi:10.1007/BF00405456

Pierella Karlusich, J. J., F. M. Ibarbalz, and C. Bowler. 2020. Phytoplankton in the Tara Ocean. Ann. Rev. Mar. Sci. **12**: 233–265. doi:10.1146/annurev-marine-010419-010706

Poulin, C., D. Antoine, and Y. Huot. 2018. Diurnal variations of the optical properties of phytoplankton in a laboratory experiment and their implication for using inherent optical properties to measure biomass. Opt. Express **26**: 711–729. doi:10.1364/oe.26.000711

Roesler, C. S., and A. H. Barnard. 2013. Optical proxy for phytoplankton biomass in the absence of photophysiology: Rethinking the absorption line height. Methods Oceanogr. **7**: 79–94. doi:10.1016/j.mio.2013.12.003

Röttgers, R., R. Doerffer, D. McKee, and W. Schönfeld. 2010. Pure water spectral absorption, scattering, and real part of refractive index model Algorithm Technical Basis Document. Univ. of Strathclyde, Glasgow, p. 1–18.

Röttgers, R., D. McKee, and S. B. Woźniak. 2013. Evaluation of scatter corrections for ac-9 absorption measurements in coastal waters. Methods Oceanogr. **7**: 21–39. doi:10.1016/j.mio.2013.11.001

Siegel, D. A., T. D. Dickey, L. Washburn, M. K. Hamilton, and B. G. Mitchell. 1989. Optical determination of particulate abundance and production variations in the oligotrophic ocean. Deep Sea Res A Oceanogr. Res. Pap. **36**: 211–222. doi:10.1016/0198-0149(89)90134-9

Simon, N., R. Barlow, D. Marie, F. Partensky, and D. Vaulot. 1994. Flow cytometry analysis of oceanic photosynthetic picoeucaryotes. J. Phycol. **30**: 922–935.

Slade, W. H., E. Boss, G. Dall'Olmo, M. R. Langner, J. Loftin, M. J. Behrenfeld, C. Roesler, and T. K. Westberry. 2010. Underway and moored methods for improving accuracy in measurement of spectral particulate absorption and attenuation. J. Atmos. Ocean. Technol. **27**: 1733–1746. doi:10.1175/2010JTECHO755.1

Sournia, A. 1975. Circadian periodicities in natural populations of marine phytoplankton, p. 325–389. *In* F. S. Russell and M. Yonge [eds.], Advances in marine biology. Academic Press.

Stramska, M., and T. D. Dickey. 1992. Variability of bio-optical properties of the upper ocean associated with diel cycles in phytoplankton population. J. Geophys. Res. Oceans **97**: 17873–17887. doi:10.1029/92JC01570

Stramski, D., and R. A. Reynolds. 1993. Diel variations in the optical properties of a marine diatom. Limnol. Oceanogr. **38**: 1347–1364. doi:10.4319/lo.1993.38.7.1347

Stramski, D., A. Shalapyonok, and R. A. Reynolds. 1995. Optical characterization of the oceanic unicellular cyanobacterium *Synechococcus* grown under a day-night cycle in natural irradiance. J. Geophys. Res. **100**: 13295–13307. doi:10.1029/95jc00452

Sullivan, J. M., and M. S. Twardowski. 2009. Angular shape of the oceanic particulate volume scattering function in the backward direction. Appl. Optics **48**: 6811–6819. doi:10.1364/AO.48.006811

Sullivan, J. M., M. S. Twardowski, J. Ronald, V. Zaneveld, and C. C. Moore. 2013. Measuring optical backscattering in water, p. 189–224. *In* A. A. Kokhanovsky [ed.], Light scattering reviews 7: Radiative transfer and optical properties of atmosphere and underlying surface. Springer.

Twardowski, M. S., E. Boss, J. B. Macdonald, W. S. Pegau, A. H. Barnard, and J. R. V. Zaneveld. 2001. A model for estimating bulk refractive index from the optical backscattering ratio and the implications for understanding particle composition in case I and case II waters. J. Geophys. Res. Oceans **106**: 14129–14142. doi:10.1029/2000JC000404

Ulloa, O., S. Sathyendranath, and T. Platt. 1994. Effect of the particle-size distribution on the backscattering ratio in seawater. Appl. Optics **33**: 7070–7077. doi:10.1364/AO.33.007070

Vaillancourt, R. D., C. W. Brown, R. R. L. Guillard, and W. M. Balch. 2004. Light backscattering properties of marine phytoplankton: Relationships to cell size, chemical composition and taxonomy. J. Plankton Res. **26**: 191–212. doi:10.1093/plankt/fbh012

Vaulot, D., and D. Marie. 1999. Diel variability of photosynthetic picoplankton in the equatorial Pacific. J. Geophys. Res. Oceans **104**: 3297–3310. doi:10.1029/98jc01333

Waterbury, J. B. 1986. Biological and ecological characterization of the marine unicellular cyanobacterium *Synechococcus*. Can. Bull. Fish. Aquat. Sci. **214**: 71–120.

Westberry, T. K., G. Dall'Olmo, E. Boss, M. J. Behrenfeld, and T. Moutin. 2010. Coherence of particulate beam attenuation and backscattering coefficients in diverse open ocean environments. Opt. Express **18**: 15419–15425. doi:10.1364/OE.18.015419

Whitmire, A. L., W. S. Pegau, L. Karp-Boss, E. Boss, and T. J. Cowles. 2010. Spectral backscattering properties of marine phytoplankton cultures. Opt. Express **18**: 15073–15093. doi:10.1364/oe.18.015073

Worden, A. Z., J. K. Nolan, and B. Palenik. 2004. Assessing the dynamics and ecology of marine picophytoplankton: The importance of the eukaryotic component. Limnol. Oceanogr. **49**: 168–179. doi:10.4319/lo.2004.49.1.0168

Yentsch, C. S., and J. H. Ryther. 1957. Short-term variations in phytoplankton chlorophyll and their significance. Limnol. Oceanogr. **2**: 140–142. doi:10.4319/lo.1957.2.2.0140

Zaneveld, J. R. V., M. J. Twardowski, A. Barnard, and M. R. Lewis. 2007. Introduction to radiative transfer. *In* R. L. Miller, C. E. Del Castillo, and B. A. Mckee [eds.], Remote Sensing of Coastal Aquatic Environments. Remote Sensing and Digital Image Processing, vol 7. Springer. doi:10.1007/978-1-4020-3100-7_1

Zhang, X., L. Hu, and M.-X. He. 2009. Scattering by pure seawater: Effect of salinity. Opt. Express **17**: 5698–5710. doi:10.1364/oe.17.005698

Acknowledgments

We thank Stephen Giovannoni and his laboratory for the use of the flow cytometer. We also thank Matthew Brown and Allen Milligan for their expertise using the LIFT-FRR. This work has benefited from discussions with Ali Chase, Carina Poulin, Allen Milligan, Robert O'Malley, the Halsey laboratory, and various participants at the 2022 Ocean Optics Conference in Vietnam. NB acknowledges that training received from the 2021 Calibration and Validation for Ocean Color Remote Sensing course, as well as support for that training by the Ocean Carbon and Biogeochemistry program, were conducive to this work. We finally thank the Editors and Reviewers for their constructive comments and criticisms that improved the presentation of this work.

Conflict of Interest

The authors declare no conflict of interests.

Submitted 05 May 2023
Revised 17 November 2023
Accepted 10 December 2023

Associate editor: Yunlin Zhang